American Mineralogist, Volume 91, pages 1941–1944, 2006

LETTER

High-pressure study of FeS, between 20 and 120 GPa, using synchrotron X-ray powder diffraction

SHIGEAKI ONO[1,*] AND TAKUMI KIKEGAWA[2]

[1]Institute for Research on Earth Evolution, Japan Agency for Marine-Earth Science and Technology, 2-15 Natsushima-cho, Yokosuka-shi, Kanagawa 237-0061, Japan
[2]High Energy Acceleration Research Organization, 1-1 Oho, Tsukuba 305-0801, Japan

ABSTRACT

Iron sulfide (FeS) has been examined in a diamond anvil cell to 120 GPa pressure using an in situ angle-dispersive X-ray diffraction technique. The transformation from a monoclinic phase (FeS III) to a newly described orthorhombic phase (FeS VI) was observed at 35–40 GPa and high temperatures. This phase remained stable during the temperature quench. After the decompression, however, the recovered sample was transformed to the troilite structure (FeS I). The relative volume change that accompanies this transformation is ~1%. No further phase transformations were observed at higher pressures up to 120 GPa, even when the sample was laser-heated to ~2000 K. There are four molecules in a single unit cell ($Z = 4$) of the orthorhombic phase. The isothermal bulk modulus (K_0) of the orthorhombic phase is 156(6) GPa, with $V_0 = 99.5(7)$ Å^3 when K_0' is fixed at 4. The *a* axis of the unit-cell parameter is more compressible than the *b* and *c* axes. Our study indicates that the phase transformation from NiAs-type (FeS V) to orthorhombic (FeS VI) phases could occur in the Martian core.

Keywords: iron sulfide, diamond anvil cell, phase transition, FeS

INTRODUCTION

High-pressure phases of FeS are of interest to planetary science because Fe-FeS alloy is thought to constitute the core of Mars based on geochemical arguments, and FeS has been found in many meteorites. (e.g., Fei et al. 1995; Kavner et al. 2001; Urakawa et al. 2004). In the case of Earth, the density of the outer core is ~10% less than the density of pure iron (Anderson and Ahrens 1994), and there is also evidence that the inner core is less dense than pure iron (Jephcoat and Olson 1987). The difference in density indicates the possible presence of a low-atomic-weight component such as H, C, N, O, Si, or S. Therefore, it is important to understand the phase stability and density of FeS at high pressures and high temperatures.

The phase stability and structural properties of high-pressure phases of FeS have been investigated by numerous previous studies (King and Prewitt 1982; Fei et al. 1995; Kusaba et al. 1998; Takele and Hearne 1999; Marshall et al. 2000; Kavner et al. 2001; Urakawa et al. 2004; Kobayashi et al. 2004). The stable phase of FeS under ambient conditions is troilite (FeS I), a superstructure of the NiAs structure. Troilite transforms to an MnP-type structure (FeS II) at 3.4 GPa and to a monoclinic structure (FeS III) at 6.7 GPa as pressure increases at room temperature. At high temperatures, troilite transforms to a hexagonal NiAs-type structure (FeS IV) and to a simple NiAs-type structure (FeS V). Kavner et al. (2001) showed that FeS III and FeS V are stable to at least 35 GPa, however pressure at the center of the Martian core is greater than 35 GPa. Accordingly, knowledge of the phase stability of FeS at extremely high pressure is important in understanding the planet's structure, dynamics, and evolution.

In this study, we conducted laser-heated diamond anvil cell experiments combined with X-rays from a synchrotron radiation source to acquire precise data on FeS phases at high pressures up to 120 GPa. We report the results of in situ X-ray powder observations of FeS and the compressibility of a new orthorhombic FeS phase identified here for the first time.

EXPERIMENTAL METHODS

The starting material, FeS (purity >99%), was purchased from Kojundo Chemical Laboratory Corporation, Japan. X-ray diffraction analysis under ambient conditions revealed that the starting material had a troilite structure (FeS I) with $a = 5.971(1)$ Å and $c = 11.682(8)$ Å. Stoichiometric FeS with the troilite structure has $a = 5.9676$ Å and $c = 11.7610$ Å (JCPDS 37-0477). A small pellet of the sample with a thickness of ~10 μm was produced using a hand press. Rhenium gaskets were preindented to a thickness of 50 μm and then drilled to give a 50 μm hole. The sample was ground to a fine powder and loaded into a diamond anvil cell (DAC) with sodium chloride as the pressure-transmitting medium. The pressure-transmitting medium remains a quasi-hydrostatic solid compared to other harder materials. Sodium chloride was also used as an internal pressure calibrant (Brown 1999; Ono et al. 2006). Synchrotron X-ray diffraction in a DAC was performed at BL13A, Photon Factory, KEK, Japan (Ono et al. 2005). The monochromatic X-ray beam was focused to less than 30 μm to minimize peak broadening caused by pressure gradients in the sample chamber. The detector-to-sample distance was calibrated using a standard CeO_2 reference sample. An angle-dispersive diffraction patterns were obtained on an imaging plate with exposure times of 10–20 min. The observed intensities on the imaging plates were integrated as a function of 2θ using the ESRF Fit2d code (Hammersley et al. 1996). The *d*-spacings of the sample and the internal pressure standard were determined by fitting a Gaussian curve to each of the diffraction peaks. The cell parameters of the samples were then calculated from the *d*-spacings with the standard deviations of the cell parameters calculated from variations in *d*-spacings. The sample was heated using a multi-mode YAG laser to induce the observed phase transformation. The typical heating time was 5–10 min at each *P-T* condition with the size of the heating spot being ~50 μm. The sample temperature was measured using the spectroradiometric method. The

* E-mail: sono@jamstec.go.jp

0003-004X/06/1112–1941$05.00/DOI: 10.2138/am.2006.2347

spectroradiometric system consisted of a thermoelectrically cooled CCD detector and a spectrograph. The use of the spectrometer allowed us to measure the temperature profile across the laser-heated spot. The temperature was determined by fitting the thermal radiation spectrum to the Planck radiation function. The system response was calibrated using a tungsten filament lamp of known radiance that was calibrated relative to a NIST standard. The radial temperature gradient in the probed region was 200–300 K. In this study, the heating temperatures were unstable, fluctuating by a couple of hundred K during the 10 minute periods at constant laser power. Therefore, the estimated temperature errors at high temperatures were about ±500 K. After each change in pressure, the sample was heated to minimize the generation of pressure inhomogeneity in the sample. After laser heating, the shape of each peak in the diffraction pattern became significantly sharper. The amount of pressure was determined from the observed unit-cell volume of B1- or B2-type sodium chloride using the equations of state of Brown (1999) and Ono et al. (2006). Equation-of-state parameters for FeS phases were obtained from pressure-volume data from the Birch-Murnaghan equation of state (Birch 1947). The determination of cell symmetry for the unknown crystal structure was performed using the Crysfire software (Shirley 2002).

RESULTS AND DISCUSSION

In the first experimental run, the sample was compressed to 60 GPa. Before laser heating, the diffraction pattern of the sample showed broad peaks reflecting compression-related differential stress. The sample was then heated to 1000–2000 K to relax the differential stress and synthesize a high-pressure phase of FeS. Following heating, the pressure decreased to 56 GPa because of stress relaxation. During the heating stage, new diffraction peaks appeared, and these remained stable after the temperature quench. The observed diffraction pattern after heating is shown in Figure 1. The new peaks could not be indexed using known high-pressure phases of FeS. This indicated that a new high-pressure phase was synthesized at 60 GPa and high temperatures.

In the second experimental run, pressure was increased directly to 120 GPa at room temperature, and the sample was then heated. After heating, the same high-pressure phase was observed. This indicates that the new high-pressure phase (FeS VI) remains stable at least up to 120 GPa, corresponding to the pressure at the core-mantle boundary in the Earth. Following decompression, the new high-pressure phase could not be recovered. The recovered sample transformed to the troilite structure (FeS I). Thus, this phase is unquenchable at ambient conditions.

In the third experimental run, the sample was gradually compressed to investigate the stability of the new high-pressure phase of FeS (FeS VI). At each pressure increment, the sample was heated to overcome transition kinetics. At 19 and 28 GPa, we observed FeS III with a monoclinic structure. When the pressure was increased to 43 GPa, however, the new high-pressure phase of FeS VI appeared. The experimental results are shown in Figure 2. Kavner et al. (2001) reported that FeS III and FeS V are stable at least to 35 GPa. According to previous studies and our current findings, the phase boundary is likely to be at ~40 GPa, however, further experiments are necessary to determine the phase relationships in FeS.

The diffraction peaks of FeS VI were reasonably indexed by an orthorhombic symmetry, and there are four molecules of this phase in a unit cell ($Z = 4$). The lattice parameters at 56.3 GPa and 300 K, for example, are $a = 5.153(3)$ Å, $b = 4.938(4)$ Å, and $c = 3.088(1)$ Å, with a unit-cell volume of 78.59(9) Å^3 for the orthorhombic cell. Table 1 shows the observed and calculated d-spacings of FeS VI.

The measured unit cell parameters and volumes are shown in Table 2. We observed that the a axis is approximately 15% more compressible than the b or c axes, which have similar compressibilities. Observed variations in the volume of FeS phases with pressure are shown in Figure 3. The pressure-volume data were used for a least-squares fit of the Birch-Murnaghan equation of state,

$$P = \frac{3}{2}K_0(x^{-7} - x^{-5})[1 + \frac{3}{4}(K_0' - 4)(x^{-2} - 1)]$$

where $x = (\frac{V}{V_0})^{\frac{1}{3}}$,

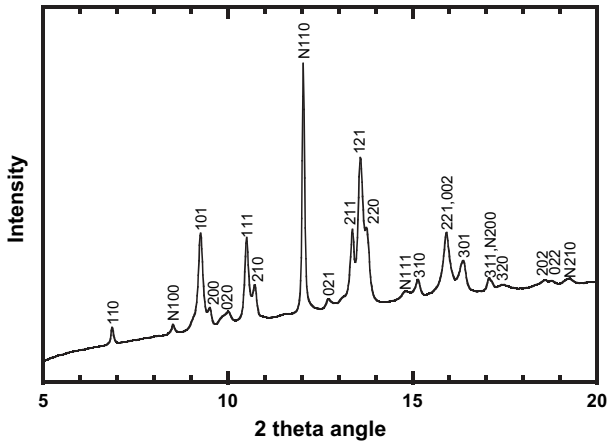

FIGURE 1. Example of diffraction pattern from FeS. These diffraction patterns were obtained at 56 GPa and room temperature. Numbers for peaks represent *hkl* values of orthorhombic phase (FeS VI). N represents B2-type NaCl. The wavelength of the monochromatic incident X-ray beam was 0.42755(5) Å.

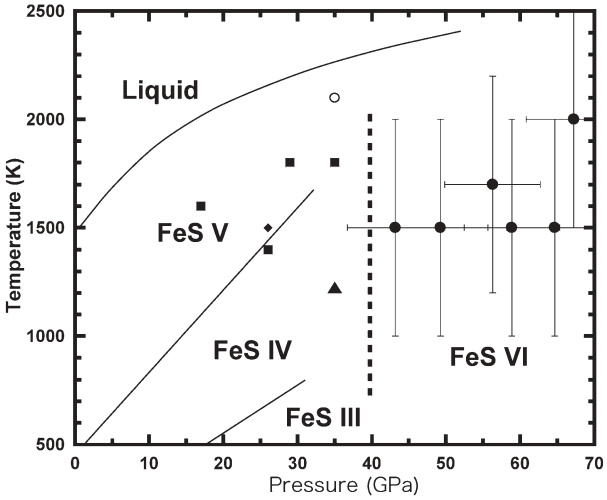

FIGURE 2. Experimental conditions and schematic phase relation of FeS. Solid circles are orthorhombic phase (FeS VI). Abbreviations of symbols reported by previous DAC study (Kavner et al. 2001) are as follows: solid squares, NiAs-type phase (FeS V); solid diamond, hexagonal phase (FeS IV); solid triangle, monoclinic phase (FeS III); open circle, melting. The phase boundaries determined by multi-anvil press experiments are shown as solid lines (Urakawa et al. 2004). A dashed line shows the inferred phase boundary.

and V_0, K_0, and K_0' are the volume, isothermal bulk modulus, and first pressure derivative of the isothermal bulk modulus, respectively. Because FeS VI could not be quenched to ambient pressure, uncertainties in V_0 and K_0' are likely to be large. Accordingly, the data were constrained by fixing K_0' equal to 4. Using all the data for FeS VI, K_0 and V_0 were 156 (6) GPa and 99.5 (7) Å^3, respectively. At 40 GPa and room temperature, the relative volume change from FeS III to FeS VI was ~1%. The molar volume of FeS VI is 24.9 Å^3 at ambient conditions, which is also smaller than those of high-*P*-*T* phases of FeS IV (27.7 Å^3) and FeS V (27.9 Å^3) at ambient conditions (Urakawa et al. 2004).

The detailed structure of the Martian interior remains an open question because of a lack of observational data. Previous high-pressure experimental studies indicate that the Martian core-mantle boundary consists of perovskite-bearing rock and sulfur-bearing iron (Fei et al. 1995; Kavner et al. 2001; Urakawa et al. 2004). Urakawa et al. (2004) estimated the Martian core pressure (36–48 GPa) for various cases, because the estimated core pressure depends on the assumed core radius, core composition and crustal thickness. If stoichiometric FeS exists in the Martian core, the stable phase could be FeS V within the outer core. As we discovered the new phase transformation in FeS at ~40 GPa, our study indicates that the Martian core may have two layers, with orthorhombic FeS VI possibly occurring at the inner core of the Mars. If seismological data can be obtained for Mars in the future, it will be possible to observe the seismic discontinuity in the Martian core related to the phase transformation from FeS V to FeS VI.

In the case of the Earth's interior, it is known from seismic observations that an ultra-low velocity zone exists at the base of the mantle. In the present experiments, we confirmed that FeS VI is stable at least up to 120 GPa. The seismic velocities of FeS VI are likely to be lower than those of the PREM model (Dziewonski and Anderson1981). Our experimental results suggest that if a small amount of iron sulfide precipitated from the core is present at the core-mantle boundary, the FeS VI contributes to a decrease in seismic velocity.

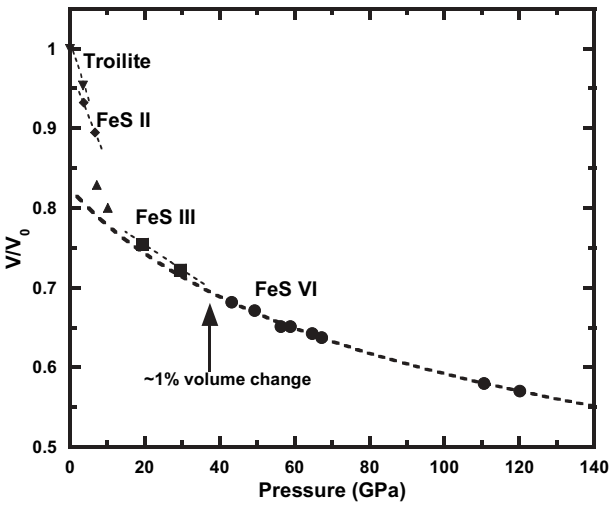

FIGURE 3. Relative volume of FeS phases as a function of pressure at room temperature. Abbreviations of symbols are as follows: solid circles, orthorhombic phase (FeS VI); solid squares, monoclinic phase (FeS III). Upper and lower triangles and diamonds are volumes of FeS phases from Nelmes et al. (1999). Dashed thick line is Birch-Murnaghan equation of state of the orthorhombic phase: K_0 = 156 (±6) GPa and V_0 = 99.49 (±0.71) Å^3 when K_0' is fixed at 4.

TABLE 1. Observed and calculated X-ray diffraction pattern of orthorhombic phase (FeS VI) at 56 GPa and room temperature

hkl	d_{obs} (Å)	d_{cal} (Å)	$(d_{obs}/d_{cal}) - 1$	I_{obs}
110	3.5673	3.5653	0.0006	12
101	2.6468	2.6491	–0.0009	67
200	2.5783	2.5765	0.0007	12
020	2.4585	2.4690	–0.0043	8
111	2.3336	2.3344	–0.0003	58
210	2.2868	2.2843	0.0011	22
021	1.9277	1.9285	–0.0004	6
211	1.8363	1.8365	–0.0001	45
121	1.8070	1.8062	0.0005	100
220	1.7851	1.7826	0.0014	47
310	1.6225	1.6223	0.0001	12
221	1.5436	1.5439	–0.0002	42
002	1.5436	1.5442	–0.0004	42
301	1.5026	1.5011	0.0010	20
311	1.4351	1.4362	–0.0008	6
320	1.4094	1.4100	–0.0004	3
202	1.3237	1.3245	–0.0007	4
022	1.3105	1.3092	0.0010	3

Note: Calculated *d*-spacings are based on orthorhombic unit-cell dimensions of a = 5.153(3) Å, b = 4.938(4) Å, c = 3.088(1) Å, and V = 78.59(9) Å^3.

TABLE 2. Lattice parameters and volumes of FeS phases to 120 GPa

P (GPa)	*a* (Å)	*b* (Å)	*c* (Å)	β (°)	*V* (Å^3)
FeS III	**monoclinic**				
19.3(1)*	7.883(6)	5.514(5)	6.293(8)	92.83(8)	273.2(5)
28.4(1)†	7.773(7)	5.428(7)	6.206(9)	92.81(8)	261.5(6)
FeS VI	**orthorhombic**				
43.2(1)†	5.234(2)	5.013(4)	3.137(2)		82.32(9)
49.3(1)†	5.199(3)	4.994(5)	3.122(2)		81.07(11)
56.3(1)†	5.153(3)	4.938(4)	3.088(1)		78.59(9)
58.9(2)†	5.148(2)	4.945(4)	3.088(2)		78.63(9)
64.7(1)†	5.119(2)	4.921(3)	3.079(1)		77.55(6)
67.2(1)†	5.115(4)	4.918(6)	3.060(2)		76.96(12)
110.6(2)†	4.934(2)	4.776(2)	2.973(1)		70.04(5)
120.1(3)†	4.903(2)	4.747(3)	2.959(1)		68.85(5)

Notes: Numbers in parentheses represent the error of lattice parameters.
* Brown (1999).
† Ono et al. (2006).

ACKNOWLEDGMENTS

Comments of an anonymous reviewer and A. Kavner helped to improve the manuscript. The synchrotron radiation experiments were performed at the PF, KEK (proposal nos. 2003G187 and 2005G122). This work was partially supported by the Ministry of Education, Culture, Sport, Science and Technology, Japan.

REFERENCES CITED

Anderson, W.W. and Ahrens, T.J. (1994) An equation of state for liquid iron and implications for the Earth's core. Journal of Geophysical Research, 99, 4273–4284.

Birch, F. (1947) Finite elastic strain of cubic crystals. Physical Review, 71, 709–824.

Brown, J.M. (1999) The NaCl pressure standard. Journal of Applied Physics, 86, 5801–5808.

Dziewonski, A.M. and Anderson, D.L. (1981) Preliminary Reference Earth Model. Physics of the Earth and Planetary Interiors, 25, 297–356.

Fei, Y., Prewitt, C.T., Mao, H.-K., and Bertka, C.M. (1995) Structure and density of FeS at high pressure and high temperature and the internal structure of Mars. Science, 268, 1892–1894.

Hammersley, A.P., Svensson, S.O., Hanfland, M., Fitch, A.N., and Häusermann, D. (1996) Two-dimensional detector software: From real detector to idealized image or two-theta scan. High Pressure Research, 14, 235–245.

Jephcoat, A. and Olson, P. (1987) In the inner core of the Earth pure iron? Nature, 325, 332–335.

Kavner, A., Duffy, T.S., and Shen, G. (2001) Phase stability and density of FeS at high pressures and temperatures: implications for the interior structure of Mars. Earth and Planetary Science Letters, 185, 25–33.

King, H.E. and Prewitt, C.T. (1982) High-pressure and high-temperature polymorphism of iron sulfide (FeS). Acta Crystallographica B, 38, 1877–1887.

Kobayashi, H., Kamimura, T., Alfè, D., Sturhahn, W., Zhao, J., and Alp, E.E. (2004) Phonon density of states and compression behavior in iron sulfide under pressure. Physical Review Letters, 93, 195503.

Kusaba, K., Syono, Y., Kikegawa, T., and Shimomura, O. (1998) High pressure and temperature behavior of FeS. Journal of Physics and Chemistry of Solids, 59, 945–950.

Marshall, W.G., Nelmes, R.J., Loveday, J.S., Klotz, S., Besson, J.M., Hamel, G., and Parise, J.B. (2000) High-pressure neutron-diffraction study of FeS. Physical Review B, 61, 11201–11204.

Nelmes, R.J., McMahon, M.I., Belmonte, S.A., and Parise, J.B. (1999) Structure of the high-pressure phase III of iron sulfide. Physical Review B, 59, 9048–9052.

Ono, S., Funakoshi, K., Nozawa, A., and Kikegawa, T. (2005) High-pressure phase transitions in SnO_2. Journal of Applied Physics, 97, 073523.

Ono, S., Kikegawa, T., and Ohishi, Y. (2006) Structural property of CsCl-type sodium chloride under pressure. Solid State Communications, 137, 517–522.

Shirley, R. (2002) The Crysfire 2002 System for Automatic Powder Indexing: User's Manual. The Lattice Press, Surrey, England.

Takele, S. and Hearne, G.R. (1999) Electrical transport, magnetism, and spin-state configurations of high-pressure phases of FeS. Physical Review B, 60, 4401–4403.

Urakawa, S., Someya, K., Terasaki, H., Katsura, Y., Yokoshi, S., Funakoshi, K., Utsumi, W., Katayama, Y., Sueda, Y., and Irifune, T. (2004) Phase relations and equations of state for FeS at high pressures and temperatures and implications for the internal structure of Mars. Physics of the Earth and Planetary Interiors, 143–144, 469–479.

MANUSCRIPT RECEIVED JUNE 15, 2006
MANUSCRIPT ACCEPTED JULY 12, 2006
MANUSCRIPT HANDLED BY BRYAN CHAKOUMAKOS